Voltage-controlled hole spin injection in nonmagnetic GaAs/AlAs resonant tunneling structures

H. B. de Carvalho,[1] Y. Galvão Gobato,[2,*] M. J. S. P. Brasil,[1] V. Lopez-Richard,[3] G. E. Marques,[2] I. Camps,[2] M. Henini,[4] L. Eaves,[4] and G. Hill[5]

[1]*Grupo de Propriedades Ópticas, Instituto de Física Gleb Wataghin, Universidade de Campinas, 13083-970 Campinas, SP, Brazil*

[2]*Departamento de Física, Universidade Federal de São Carlos, 13560-905 São Carlos, SP, Brazil*

[3]*Faculdade de Filosofia Ciências e Letras de Ribeirão Preto, Departamento de Física e Matemática, Universidade de São Paulo, 14040-901 Ribeirão Preto, SP, Brazil*

[4]*School of Physics and Astronomy, University of Nottingham, NG7 2RD Nottingham, United Kingdom*

[5]*EPSRC National Centre for III-V Technologies, University of Sheffield, Mappin Street, Sheffield S1 3JD, United Kingdom*

(Received 14 November 2005; revised manuscript received 19 January 2006; published 18 April 2006)

We have investigated polarization-resolved photoluminescence under applied voltage in *p-i-p* GaAs/AlAs double-barrier diodes. We have observed oscillations in the *degree of polarization* up to 36% at $B=15$ T with sign reversals occurring near to the hole subband resonances. At high voltages a polarization saturation up to 25% at $B=15$ T is observed. The data are interpreted by using simulations based on a simple theoretical model that considers spin conservation for tunneling and the relaxation processes for carriers at Zeeman states in the quantum well. Our work offers the prospect for the development of voltage-controlled spin filtering systems using standard nonmagnetic semiconductor heterostructures.

DOI: 10.1103/PhysRevB.73.155317 PACS number(s): 78.67.De, 72.25.Dc, 78.55.−m, 78.66.−w

I. INTRODUCTION

There is great interest in the manipulation of spin degrees of freedom in semiconductor devices for applications in spintronics.[1–5] These systems can combine the advantage of long spin lifetimes and well-defined polarization of the emitted light with the flexibility of external carrier population control and high mobilities. In this context, the resonant tunneling effect has proved to be an important tool for the spectroscopy of new physical phenomena such as the manipulation of spin polarization. Recently, the successful operation of a semimagnetic resonant tunneling diode (RTD) as a voltage-controlled electron-spin-polarized filter was reported.[6] Using a complex multilayer structure, Fiederling *et al.*[7] demonstrated light-emitting diodes using spin-polarized injection of electrons from semimagnetic II-VI semiconductor layers.

The spin polarization of two-dimensional (2D) hole systems has also attracted great interest[8–10] recently. The strong interaction between the energy branches in the valence band results in highly nonparabolic dispersions and in large and anomalous *g* factors, in contrast to the almost parabolic dispersions and small *g* factors observed in the conduction band of wide-gap semiconductors. Measurements of *g* factors for carriers in a GaAs-AlGaAs quantum well (QW) have been performed by electron spin resonance,[11] Hanle effect,[14] time-resolved photoluminescence[12] (PL), and spin-flip Raman scattering experiments.[13] Most of the work in this area has been devoted to the determination of electron *g* factors in GaAs-AlGaAs as a function of well width, Al concentration, and crystalline growth direction.[14–16] For QW widths above 15 nm, a *g* factor close to the bulk value (−0.44) has been observed. This increases for narrower wells and passes through zero near 5.5 nm. Much less information is available for hole *g*-factor values which are strongly anisotropic and dependent on the type of confinement.[12,13] Measurements of the heavy-hole ground-state (HH_1) *g* factor showed a large difference between magnetic field applied parallel [$g_{\parallel}=+2.3$ (Ref. 13)] and perpendicular [$g_{\perp}=+0.04$ (Ref. 12)] to the growth axis in single GaAs-AlGaAs quantum wells.[17] Hole *g* factors are also very sensitive to the coupling between hole subbands; therefore, the values for excited heavy- and light-hole states should also vary significantly.

Another point of interest is the hole spin relaxation times. It is usually accepted that bulk holes (3D system) lose their spin polarization quasi-instantaneously.[18] However, spin relaxation times for confined holes (low-dimensional systems) become significantly larger, due to changes in the valence band structure caused by the stronger coupling in confined regimes. The reported spin relaxation times range from 4 ps to 1 ns, depending on the structure design and on the experimental conditions.[19–24] These reports of large and anomalous *g* factors and long spin relaxation times lead us to conclude that RTD's are interesting systems to study spin polarization effects in quasi-2D hole gases since there is the possibility of varying the population of carrier levels using external voltages, with the system maintaining spin polarization for relatively long time scales.

We report on measurements of polarization-resolved photoluminescence under applied voltage in a nonmagnetic *p-i-p* GaAs/AlAs RTD, where a minority concentration of electrons is photogenerated far from the quantum well layer. The magnetic field applied perpendicular to the plane of the GaAs well layer leads to the Zeeman splitting of both electron and hole quasi-two-dimensional levels of the QW. The spin-dependent tunneling and energy (momentum) relaxation of injected carriers were investigated by analyzing the bias dependence of left (σ^-) and right (σ^+) circularly polarized PL from the QW states, as shown schematically in Fig. 1. We have observed that the polarized PL spectra are highly bias sensitive, with their *degree of polarization* showing two distinct regimes. In the low-voltage regime (below 1 V in this sample) the polarization of the optical emission lines exhibits

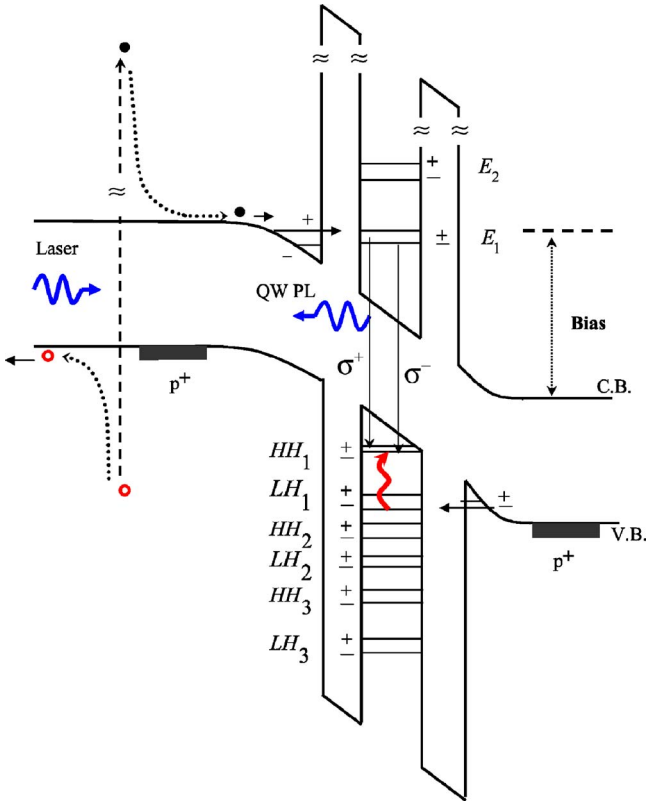

FIG. 1. (Color online) Schematic band diagram including spin-split levels, intraband optical transitions, and carrier injections under applied bias and magnetic field. The spin polarization of states in each spatial localization region are represented by (−) and (+). Excitation occurs far away from the double barrier.

sign inversions near the resonant hole peaks of the tunneling current. In the high-voltage regime (above 1 V in this sample) the polarization increases with increasing bias to a saturation value. In order to analyze and interpret the main aspects of these experimental results, we have developed a simple theoretical model based on spin conservation during tunneling and during the energy relaxation of carriers.

The paper is organized as follows: in the next section we describe the experimental setup and present the main results; in Sec. III, we introduce the details of the theoretical model based on the spin-sensitive carrier injection and relaxation mechanisms; finally, in Sec. IV, we compare our theoretical findings with experiments and discuss the main implications of the work.

II. EXPERIMENT

The structure used in this work is a symmetric *p-i-p* GaAs/AlAs RTD, similar to that previously used to probe the strongly admixed valence subbands of the GaAs QW using magnetotunneling spectroscopy[25] and to study the effect of hole space-charge buildup on the resonant peaks.[30,31] The device comprises the following layers in order of growth from the top of a GaAs substrate: 3-μm-thick Be-doped GaAs ($p=2\times10^{18}$ cm^{-3}) lower contact layer, 100 nm GaAs ($p=1\times10^{18}$ cm^{-3}), 100 nm GaAs ($p=5\times10^{17}$ cm^{-3}), 5.1-nm undoped GaAs spacer layer, 5.1-nm undoped AlAs barrier, 4.2-nm undoped GaAs quantum well, 5.1-nm undoped AlAs barrier, 5.1-nm undoped GaAs spacer layer, 100 nm GaAs ($p=5\times10^{17}$ cm^{-3}), 100 nm GaAs ($p=1\times10^{18}$ cm^{-3}), and GaAs top contact layer, 0.6-μm ($p=2\times10^{18}$ cm^{-3}) top contact layer. The structure was processed into 400-μm-diam mesas with a metallic AuGe annular top contact to provide access for optical measurements under applied bias. The sample was mounted in a superconductor magnet, and the photoluminescence spectra were recorded using a double spectrometer coupled to a charge-coupled-device (CCD) system and polarization optics to select σ^+ and σ^- configurations. The left and right circular polarizations were unequivocally defined based on the Zeeman splitting of bulk near-band-edge GaAs emission for which the sign of the corresponding g factor is well known. An Ar^+-ion laser was used as the excitation power source to generate minority electrons close to the surface of the top GaAs layer.[32] We have used linearly polarized 488 nm light from the Ar^+ laser; therefore, spin polarization of carriers by laser excitation is not expected. The schematic potential energy profile of the structure, under bias and magnetic field, is shown in Fig. 1, where a majority (minority) hole (electron) 2D accumulation layer is formed on the positive- (negative-) biased side, adjacent to the right (left) interface barrier. At zero bias, no QW emission was detected in this sample. This indicates that the amount of light that reaches the QW and probably AlAs layer is negligible in our experimental conditions. As the bias is continuously increased, the alignment of each spin-split energy level of carriers in the injector layers with a split subband of the QW layer produces a resonant peak in the tunnel current. The current in our sample has two contributions, one from minority electrons and the other from majority holes tunneling through the diode. Figure 2(a) shows the *I-V* characteristics (solid line) for a field $B=15$ T applied parallel to the current with the main hole peak positions shown on the top axis. The sequence is according to Ref. 25. We observe a sensitivity of the PL with voltage, in particular the strong oscillatory behavior of the *degree of polarization* at low bias. This arises from a combination of selection rules (see Fig. 1) governing the spin-dependent recombination of electrons and holes and from the change induced in the population of the spin-split QW ground states, via bias sweeping.

In order to analyze the spin polarization of electrons and holes tunneling into the QW layer as well as the charge buildup in the ground-state subbands, we have performed circularly polarized PL measurements as a function of applied bias. Figure 2(b) shows some specific circularly polarized PL spectra taken at the voltages $(V_1,\ldots,V_5)$ marked in panel (a). Note how the PL intensity changes with external bias, an indication of how the ground-state populations inside the QW are changing due to carrier injection. More specific information can be obtained from the *degree of polarization* measured at each voltage (V); this is defined as

$$\mathrm{pol}(V)=(I^{\sigma^+}-I^{\sigma^-})/(I^{\sigma^+}+I^{\sigma^-}), \tag{1}$$

where I^{σ^+} and I^{σ^-} are the integrated PL intensities for each polarized spectrum. The bias dependence of this quantity is

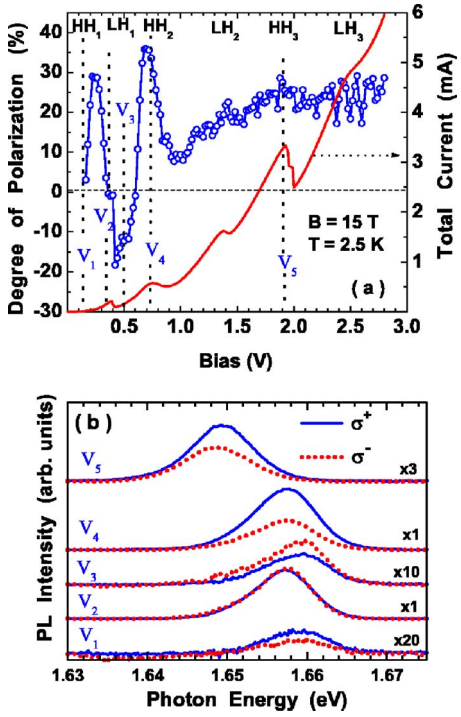

FIG. 2. (Color online) (a) The current-voltage characteristics (solid line) under light excitation and the degree of polarization [pol(V)] of the quantum well optical emissions (open circles), for $B=15$ T, shown as a function of applied bias. (b) Typical σ^+ (solid line) and σ^- (dotted line) PL spectra, taken at the marked voltages in panel (a). For clarity, the spectra were multiplied by different factors shown in the left.

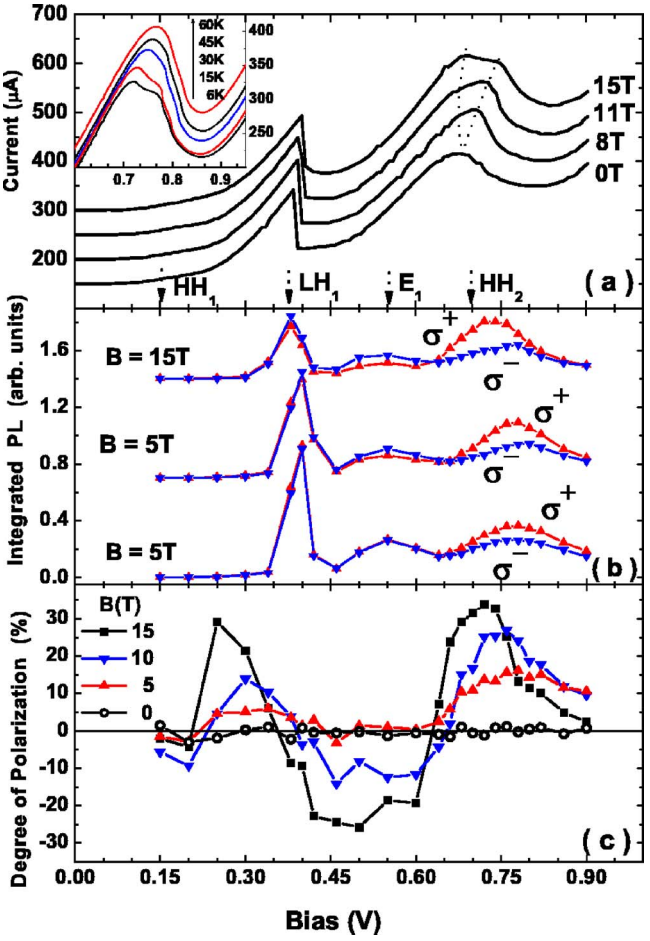

FIG. 3. (Color online) (a) The current-voltage characteristics in the low-voltage regime. For clarity, the $B=0$ curve is shown with 150 μA offset and the subsequent ones with 50 μA. Note the magnetic enhancement of the HH_2 spin states. The inset shows (without offset) how the HH_2 doublet structure is washed out by thermalization above $T=45$ K, for $B=15$ T. (b) The σ^+ (up-triangles) and σ^- (down-triangles) integrated PL intensities versus voltage for $B=5$, 10, and $B=15$ T. (c) pol(V) for different values of B.

also shown in Fig. 2(a). There are two distinct regimes of optical polarization. For the low-voltage regime, below 1 V for this sample, pol(V) has an oscillatory behavior with peak values of up to 36%. Also, we observe sign reversal near each resonant peak of the tunnel current. In the high-voltage regime above 1 V, the optical polarization shows a saturation value [pol(V) $\sim 25\%$].

Let us analyze more closely the low-voltage regime. Figure 3(a) shows I-V curves, measured at a temperature of 2.5 K, for different values of magnetic field. For clarity, the $B=0$ curve has 150 μA offset and the subsequent ones, 50 μA. Three hole resonant peaks appear in this figure, and their critical voltages were assigned on the basis of our previous work[25] to the following subbands: the first one is a heavy-hole (HH_1) resonance with a very small shoulder, occurring at 0.15 V; it is shown at higher resolution in Ref. 25. The next peaks are the first light-hole resonance (LH_1) at 0.37 V and the second heavy-hole resonance (HH_2) at 0.70 V. As shown schematically in Fig. 1, the B field plus spatial confinement split the levels in the QW and in the injector layers into *spin-up* and *spin-down* Zeeman states. It is expected, however, that the Zeeman energy separations in the accumulation layer and in the QW layer assume different values (g factors) due to their distinct confinement potential and subband mixing. Note that in high magnetic fields, the HH_2 resonance shows changes that could be associated with tunneling through distinct Zeeman-split states. As will be discussed later, a possible explanation for the observed change is related by the difference between g factors in the accumulation and QW layers. In the inset in Fig. 3(a) we show the effect of increasing temperature on the shape of this double-peak structure. It is observed that near $T=45$ K, the doublet structure of the HH_2 resonance is washed out by thermal excitations, providing a possible corroboration of our assignment.

The I-V data are complemented by the PL measurements which provide more information about the electronic structure. The integrated PL intensities of the σ^+ (up-triangles) and σ^- (down-triangles) components are presented in Fig. 3(b) as a function of the voltage for $B=5$, 10, and 15 T. The sensitivity of the optical polarization is evident in Fig. 3.

As can be seen from Fig. 3(b) there are two strong peaks which correspond to the LH_1 and HH_2 resonances in the I-V curve. In addition, a small peak is observed at 0.55 V. This third contribution, not observed in the I-V characteristics but observed in photocurrent measurements, corresponds

to the maximum occupation of the E_1 QW level by the resonant injection of the photogenerated electrons. The main reason why this electron resonance is not observed in Fig. 2(a) is because the total current is proportional to the sum of hole and electron densities ($d_{cond}+d_{val}$) and, for our experimental power generation conditions, we have $d_{cond} \ll d_{val}$. In contrast, the PL intensity is proportional to the product ($d_{cond} \times d_{val}$) and, therefore, is much more sensitive to any charge buildup variation in the conduction or valence band levels, hence the resulting strong modulation of the PL emission near the resonant voltage for electrons tunneling into the E_1 QW level.

We emphasize that at zero bias no QW emission was detected in this sample. This demonstrates that the amount of light absorbed in the QW layer is negligible in our experimental condition. For $V>0$, holes and electrons start to enter the QW via tunneling into the respective subband levels and then the polarized σ^+ and σ^- PL emissions are observed. These emissions correspond to excitonic transitions between the $E_1^{\pm}$ and $HH_1^{\pm}$ spin-split ground states of the QW, as shown schematically in Fig. 1. Furthermore, they correspond to E_1-HH_1 recombination even when the device is biased for resonant tunneling of holes via higher energy states $LH_1^{\pm}$, $HH_2^{\pm}$,... of the QW (see Fig. 1). We were not able to detect any PL from excited electron and hole QW subbands, such as E_1-LH_1, for instance.

We observed that the σ^+ and σ^- PL peaks show negligible energy splitting in the low-voltage regime as seen in curves $V_1,\ldots,V_4$ in Fig. 2(b). This implies a null g factor for these excitonic transitions where $g^{ex}=g_e+3g_h$ (Ref 26); the multiplying factor of 3 comes from the total spin component of heavy holes $\left(\frac{3}{2},\pm\frac{3}{2}\right)$. Thus, the value $g^{ex}=0$ detected in our experiments implies that the values for unbound (free) electron (E_1-branch) and hole (H_1-branch) carriers obey the relation $g_e=-3g_h$. This value for a RTD structure is much smaller than that reported in Ref. 15 for an isolated QW with a similar well width. The reason for this difference is associated with the delocalized nature of the states in the RTD in contrast to the localized nature for a QW. For the high-voltage regime, the σ^+ and σ^- PL peak energy separation shows a small splitting [see curve V_5 of Fig. 2(b)] that depends on the applied voltage. Using a Gaussian fitting, the highest detected splitting in our sample was 0.8 meV at 1.90 V. This effect is attributed to the electric-field-induced spin-orbit, Stark, and interband coupling contributions to the effective Zeeman splitting of holes and electrons.[27]

The line for $B=0$ T (open circles), in Fig. 3(c), shows that the *spin-up* and *spin-down* ground states remain degenerate and there is no detectable difference in the population of electrons and holes in the low-voltage regime. Figure 3(b), for 5, 10, and 15 T, shows that the integrated PL intensities are sensitive to changes in the *spin-up* and *spin-down* ground-state populations, as the bias increases.

The PL intensities near the critical voltage for HH_1 split states ($\sim$0.15 V) is very small because, at this low voltage, the probability for injecting holes directly into HH_1 and E_1 states becomes small. Note that the electrons involved in the optical transition in the range of voltage ($<$0.5 V) are injected out of resonance. As the voltage increases, the number of positive and negative charges tunneling into a high-energy level and relaxing to the HH_1 and E_1 spin-split states increases and thus the integrated PL intensities also increase. It is interesting to note from Fig. 3(b) the increase of the σ^+ and σ^- PL intensity resolution near E_1 ($\sim$0.55 V) and HH_2 ($\sim$0.75 V) resonant voltages, as the magnetic field increases.

Figure 3(c) shows the dependence of the optical degree of polarization with bias applied to the structure for different values of the magnetic field. We draw attention to the high sensitivity of pol(V) to the changes in the population of the electron and hole ground states. An interesting feature of the data is that pol(V) exhibits sign inversions as the voltage is swept near the hole resonances and, for $B=15$ T, the polarization reaches 36% near the $HH_2^{\pm}$ resonant voltage. As already mentioned, these emissions come from E_1-HH_1 recombination and the dipole optical transitions between $E_1^+ \Leftrightarrow HH_1^+$ and $E_1^- \Leftrightarrow HH_1^-$ states are governed by strict selection rules. The sign inversion of pol(V) is associated with the change in the population of $HH_1^{\pm}$ and $E_1^{\pm}$ states, when the bias sweeps through any resonant state [see Fig. 2(b)]. A saturation of pol(V) is observed at high applied bias. In the next section we discuss how this saturation can be explained in terms of the spin-selective increase of the QW escape rates at high voltage along with thermalization processes.

In the next section, we present a theoretical model to explain in a more quantitative way our experimental data.

III. THEORETICAL MODEL

To analyze our experimental results we have developed a model to calculate the PL spectra and polarization in a RTD based on the following ideas. The degree of polarization for the $E_1^{\pm} \Leftrightarrow HH_1^{\pm}$ emissions may be produced by two main effects: (i) the preferential occupation of $E_1^{\pm}$ or $HH_1^{\pm}$ spin ground states in the QW following thermal redistribution over these two lowest-energy QW Zeeman-split states and (ii) the preferential spin-polarized injection of carriers directly into the QW spin-type states. Both effects require the existence of energy relaxation mechanisms when a carrier is injected into a high-energy level (high k-vector energy branch or Landau level) of the conduction or the valence bands, E_n, HH_n, and LH_n, $n=1,2,\ldots$ states, respectively.

Case (i) becomes dominant for spin-unpolarized injection of carriers or for spin-polarized injection but when the spin-coherence time of carriers is smaller than other relevant time scales such as tunneling, relaxation, and optical recombination times. In contrast, the second case may become dominant when at least one of the injected carrier types is spin polarized and its spin-coherence time is larger than the other time scales involved.

Case (i) does not apply to our experiments since thermal excitations and spin-flip processes would be efficient spin-depolarizing mechanisms for the carriers entering the $HH_1^{\pm}$ and $E_1^{\pm}$ states. Furthermore, any residual optical degree of polarization for case (i) should remain roughly constant as the bias increases. The lack of a thermal redistribution of carriers is evident from Fig. 3(a) where the splitting of the $HH_2^{\pm}$ resonances is clearly resolved at $B=15$ T. Here the

spin-split related peaks have slightly different height, indicating no significant thermalization of carriers at $T=2.5$ K. For small B fields—that is, smaller Zeeman splitting—the polarization is observed at the same temperature which indicates the absence of a thermal depolarization effect. As the temperature increases the energy splitting of the HH_2 doublet peak is smeared out and, above $T\sim 45$ K as shown in the inset of Fig. 3(a), the spin-depolarization thermal processes become activated.

As discussed in the Introduction, hole spin relaxation times may become quite large for GaAs quasi-2D states in the presence of a magnetic field.[19–24] We conclude that in our sample, the optical polarization is due to the injection of spin-polarized carriers into the QW and that they maintain their spin polarization during tunneling and during energy relaxation processes, corresponding to case (ii). Based on these facts, we also conclude that the spin-coherence times of injected carriers are larger than the tunneling and energy relaxation times, a necessary condition to observe spin-polarized emissions in the system at all bias.

Furthermore, the detection of ground-state σ^+ and σ^- PL emissions at all voltages requires that a fraction of the holes injected into the high-energy states should relax to the $HH_1^{\pm}$ and $E_1^{\pm}$ energy states, before recombination. It is known that electron-phonon interaction Hamiltonians are independent of the spin degree of freedom. The other possible *spin-flip* scattering mechanism, as studied by D'yakonov and Perel,[28] may lead to spin depolarization during relaxation. The *spin-flip* relaxation time τ_{SF} is proportional to the reciprocal of the square of the spin-splitting energy (ΔE_{Zy}) and the typical momentum (energy) scattering time via phonons (τ_{ph}). This gives $\tau_{SF}^{-1}=(\tau_{ph}/2)[\Delta E_{Zy}/\hbar]^2$. However, the considerably higher degree of optical polarization observed in our experiments is strong evidence for carrier energy relaxation occurring through spin-preserving phonon emission processes. Furthermore, for the low-voltage regime, any contribution due to spin-orbit interaction can be neglected. However, for the high-voltage regime, where local electric fields are large, at least the Rashba spin-orbit contribution may play a role whereas the spin-orbit parameter for the Dresselhaus term is small[29] for the GaAs layer. This effect will be considered here only as an effective renormalization of the Landé g factors. Therefore, we do not include any *spin-flip* relaxation process in our model.

Our theoretical model is therefore based on the following processes: (i) e-h pair recombination that generates the PL; (ii) efficient spin-sensitive tunnel injection of holes into a QW state of any energy (k-vector or B-dependent) $HH_n^{\pm}$ and $LH_n^{\pm}$ followed by a spin-conserving energy relaxation to $HH_1^{\pm}$ ground states; (iii) efficient spin-sensitive tunnel injection of electrons into the $E_n^{\pm}$ states, with a spin-conserving energy relaxation to $E_1^{\pm}$ ground states; and (iv) voltage-dependent probability of escape of carriers from the QW, via tunneling through the second barrier.

By including these effects on the carrier dynamics in the conduction and valence QW subbands, the PL intensity, as a function of the emitted light frequency ω, is calculated as

$$I^{\sigma^s}(\omega) = -D\sum_j \mathrm{Im}\left\{\frac{|P_j^s|^2(1-n_{val_j}^s)n_{cond_j}^s}{\hbar\omega-\Delta E_j+i\delta_j}\right\}, \qquad (2)$$

where $D=(eB)/(2\pi\hbar)$ is the spin-split Landau-level degeneracy per unit area.

The j sum runs over all possible dipole transitions connecting conduction ($|\mathrm{cond}_j\rangle$) and valence ($|\mathrm{val}_j\rangle$) bands allowed by optical selection rules that determine the oscillator strengths $|P_j^s|=|\langle \mathrm{cond}_j|\sigma^s p|\mathrm{val}_j\rangle|$. Here σ^s defines the circular polarization of the emitted light and δ_j is the line broadening for each excitonic optical transition.

The electron *occupation function* probability determining the charge buildup in the valence (E_{val_l}) and conduction (E_{cond_l}) band levels is represented by n_{val}^s and n_{cond}^s, respectively. In the presence of a field B, the optical transition energy ΔE_j becomes $\Delta E_{l,N}=E_{cond_l}-E_{val_l}-\Delta E_{ex}+(N+1/2)\hbar\Delta\omega_{l,N}+s(g_j^{ex}\mu_B/2)B+\Delta E_{diamag}$, where $\Delta\omega_{l,N}=eB/c[1/m_{cond_l}-1/m_{val_l}]$ is the electron-hole (e-h) cyclotron frequency difference for the level l, N is the Landau level index, $s=\pm$, g_j^{ex} is the effective excitonic Landé g factor of the resonant levels involved, ΔE_{ex} is the QW exciton-binding energy, and ΔE_{diamag} is a diamagnetic correction. We use the weak-Coulomb-binding approximation in which the excitons can be described as weakly coupled e-h pairs.

The summation can be dropped for our present experimental condition in which only one PL line with σ^+ or σ^- polarization is detected [see Fig. 2(b)]. Therefore, the electron occupation probability in the spin-polarized valence band ground state is calculated as $n_{\mathrm{HH}_1}^s=1-\Sigma_\alpha p_\alpha^s\pi_\alpha^s$, where p_α^s is the voltage-dependent density of holes with spin s injected into a QW state α ($\alpha=\mathrm{HH}_1^s,\mathrm{HH}_2^s,\ldots,\mathrm{LH}_1^s,\mathrm{LH}_2^s,\ldots$) and π_α^s is the annihilation rate between electrons in the upper valence band level and holes in the state α. Analogously, the electron occupation probability of the conduction band ground state involved in the optical recombination is given by $n_{E_1}^s=\Sigma_\beta n_\beta^s\pi_\beta^s$, for our sample which has two QW conduction subbands, $\beta=E_1^s$, E_2^s. In the model, these injected carriers may either undergo an energy relaxation process described by a probability $\pi_{\alpha(\beta)}^s$ which favors the luminescence or be ejected from the α-valence (β-conduction) band state, with a probability ζ_α^s (ζ_β^s). Charge conservation requires that $\pi_{\alpha(\beta)}^s+\zeta_{\alpha(\beta)}^s=1$ in the valence (conduction) band.

In order to describe the density of injected electrons and holes, we have constructed a model derived from the I-V characteristics of the sample. The *occupation function* probability of a spin-polarized hole state depends on the voltage drop V_d between the accumulation layer and the QW level, which aligns the Fermi level in the accumulation layer to the QW hole subband, according to the following relation:

$$p_\alpha^s(V_d)=\nu_\alpha^s\frac{\Gamma_\alpha^2}{(eV_d-\Delta E_\alpha-s\mu_B\Delta g_\alpha B/2)^2+\Gamma_\alpha^2}, \qquad (3)$$

where $\Delta E_\alpha+s\mu_B\Delta g_\alpha B/2$ is the difference between the energy of a hole state α ($\alpha=\mathrm{HH}_1^s,\mathrm{HH}_2^s,\ldots,\mathrm{LH}_1^s,\mathrm{LH}_2^s,\ldots$) inside the QW and the energy of the hole ground state (HH_1^s) in the accumulation layer both with same spin polarization s; Δg_α

is the difference between the g factors of these two related states. The Zeeman term has been kept explicit in order to highlight the spin-dependent injection, whereas the Landau-level dependence, proportional to the cyclotron frequency difference between the QW and the accumulation layer, is implicit in ΔE_α. We consider a Fermi-level filling only the HH_1 state in the hole injector layer (see Fig. 1). Also, ν_α^s is a relative level *filling* for the QW-hole-split level in the presence of field B which defines the occupation in a given valence Landau state due to the charge density injected from the accumulation layer. The Kronecker-like δ function, which characterizes the accumulation layer and QW-level alignment, has been modified through the introduction of an effective lifetime broadening Γ_α. Each hole resonant peak in the I-V characteristics is associated with the voltage drop V_d, which defines the value of ΔE_α for the sample. The relation between the external bias V applied across the entire device and this local voltage drop V_d will be discussed below.

In a similar way, the *occupation function* probability determining the charge buildup of the injected polarized electrons can be defined as

$$n_\beta^s(V_d) = \nu_\beta^s \frac{\Gamma_\beta^2}{(eV_d - \Delta E_\beta - s\mu_B \Delta g_\beta B/2)^2 + \Gamma_\beta^2}, \tag{4}$$

where $\Delta E_\beta + s\mu_B \Delta g_\beta B/2$, Γ_β, s, ΔE_β, and eV_d have the equivalent meanings for the conduction band as in Eq. (3) for the valence band; since electrons are photogenerated, ν_β^s is proportional to the optical excitation intensity and depends smoothly on the external voltage.

Including all the processes responsible for the charge buildup in the QW layer, the PL intensity as a function of the emitted light frequency ω for different transitions is given by

$$I_{PL}^{\sigma^s}(\omega) = D \sum_{\alpha,\beta} \frac{|P^s|^2 \delta_{1,0} [p_\alpha^s (1 - \zeta_\alpha^s) n_\beta^s (1 - \zeta_\beta^s)]}{[\hbar\omega - \Delta E_{1,0}]^2 + \delta_{1,0}^2}. \tag{5}$$

It can be seen from this relation that $I_{PL}^{\sigma^s}(\omega)$ is given by the sum of the linewidth of the electron (Γ_β) and hole (Γ_α) states involved on the optical transitions. Note also the dependence on the injected densities (p_α^s and n_β^s) and on the escape probabilities ζ_α^s and ζ_β^s.

Finally, the integrated PL emission for each polarization, as a function of applied bias, can be calculated from the above equation and becomes

$$I^{\sigma^s}(V_d) = \pi D |P^s|^2 \sum_{\alpha,\beta} p_\alpha^s(V_d)(1 - \zeta_\alpha^s) n_\beta^s(V_d)(1 - \zeta_\beta^s). \tag{6}$$

It is interesting to note that the level lifetime dependence remains only in the occupation functions defined in Eqs. (3) and (4). Therefore, the optical degree of polarization pol(V) can be calculated directly from Eq. (6). However, pol(V) depends on the local voltage drop V_d which requires us to establish one relation between applied bias V and V_d.

The energy drop of a level in the QW region, eV_d, is proportional to the total external bias V in the form

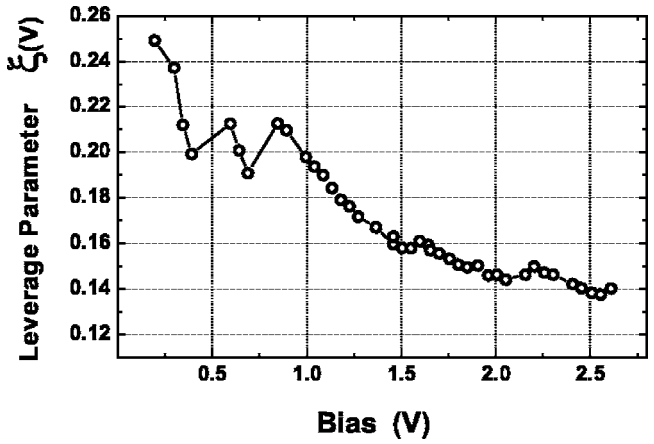

FIG. 4. Electrostatic leverage factor establishing the relation between the total voltage (bias) V applied to the entire sample and the voltage drop V_d causing the alignment between the QW subband levels and the injector layer level, taken from Ref. 30.

$$V_d = \xi V, \tag{7}$$

where the electrostatic leverage parameter ξ depends on the composition of the sample and on the space-charge distribution. Reference 30 describes a model to extract the 2D charge buildup in the QW levels of the same sample that is studied here. The dependence of ξ on the applied bias is shown in Fig. 4. In a zeroth-order approximation ξ may considered as independent of V; the mean value is $\xi_0 = 0.17$ for this sample. In the next section, we determine the unknown parameters $\Delta g_\alpha(\beta)$ and $\Gamma_{\alpha(\beta)}$, $\alpha = HH_1, HH_2, \ldots, LH_1, LH_2, \ldots$ ($\beta = E_1, E_2$) using the V-dependent value $\xi(V)$ in our numerical simulation; the electrostatic leverage parameter simply rescales the values of Δg's and Γ's.

IV. RESULTS AND DISCUSSION

Our model describes the optical polarization in the low- and high-voltage regimes according to the strength of the QW escape probabilities ζ_α^s and ζ_β^s as compared to unity. In the low-voltage regime these probabilities are very small ($\zeta_\alpha^s \ll 1$, $\zeta_\beta^s \ll 1$) due to the large barrier height (see Fig 1). In this bias range the integrated PL intensities are determined mainly by the spin-selective electron- and hole-injected concentrations into the QW. For the high-voltage regime, the effective barrier heights for tunneling out of the QW become lower and the escape probabilities increase. Therefore, the integrated intensity should decrease [see Fig. 5(b)] in the high-bias region.

Figure 5(a) shows a comparison between σ^+ (up-triangles) and σ^- (down-triangles) experimental integrated intensities of the PL spectra and the theoretical simulation (solid lines) obtained with our model, for $B = 15$ T over the entire bias range. The vertical arrows in Fig. 5(a) label the positions of the main resonant voltages. The overall agreement for each polarization is quite satisfactory. It is interesting to note the weak PL intensities near the electron resonance E_1 as well as in the high-voltage regime near the HH_3 and LH_3 spin-split doublets. The electron resonant tunneling condition at

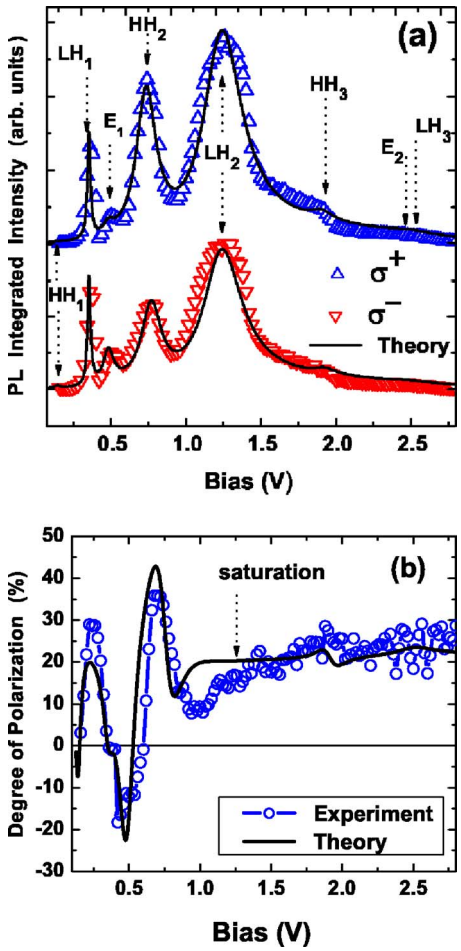

FIG. 5. (Color online) (a) Theoretical (solid line) and experimental integrated PL intensity for σ^+ (up-triangles) and for σ^- (up-triangles) configurations, as functions of bias. (b) Comparison between calculated (solid line) and experimental (symbol) degrees of polarization as functions of bias. In both cases, the magnetic field is $B=15$ T.

0.55 V takes place between the LH_1 and HH_2 resonances which, inevitably, will interfere in the final emission intensities due to the line broadening effects and, more important, to the off-resonance injection condition of these two hole states that are populating the HH_1 doublet, after energy relaxation.

Figure 5(b) compares the calculated degree of polarization (solid line) with the experimental data (symbols). Note that in the low-voltage regime, the optical polarization shows sign inversion each time the injector level crosses the spin-doublet structure of a QW subband. The measurements show clearly that the optical emission from the QW is a sensitive mechanism able to probe very small changes in the relative population of the spin-split states.

It is interesting to note that the strong (LH_2) as well as the two very weak (HH_3 and LH_3) resonant emissions for σ^+ and σ^- configurations in the high-voltage regime ($V>1.0$ V) [Fig. 5(a)] have positive values for the optical degree of polarization. Moreover, pol(V) increases to the saturation value pol(V)$\sim+25\%$. Note that for voltages near E_2, HH_3, and LH_3 resonances, the approximations $\zeta_\beta^s \ll 1$ and $\zeta_\alpha^s \ll 1$ no longer hold. For this regime, the applied voltage has reduced the effective QW barrier heights to a condition in which the carriers arriving into these levels escape more easily from the QW; thus, the fraction relaxing to E_1 or to HH_1 ground levels decreases, so that the polarized PL intensities show weak peaks since the population in each spin-split ground level becomes very small. Our theoretical model reproduces this imbalance between the spin-state populations via the terms $n_{E_2}^+(V_d)(1-\zeta_{E_2}^+)$ and $n_{E_2}^-(V_d)(1-\zeta_{E_2}^-)$ in the conduction band. Similar terms for the valence band contribute to the sum in Eq. (6). Note that the higher the energy level inside the QW, the lower is the occupation provided to the ground-level population.

TABLE I. Parameters determined from the theoretical simulation model.

QW state	$\xi(V)$	Γ [meV]	Δg
E_1	0.20	8.20	0.0
E_2	0.15	122.86	0.018
HH_1	0.25	5.00	0.0
LH_1	0.22	2.64	0.25
HH_2	0.19	15.01	7.66
LH_2	0.20	31.2	0.24
HH_3	0.15	13.50	3.46
LH_3	0.14	21.60	6.63

Table I shows the set of parameters that best reproduce the experimental data in our simulation model. We have used the V-dependent electrostatic leverage parameter $\xi(V)$ (Fig. 4) to determine the local voltage drop V_d.

Two points need to be considered when analyzing this set of parameters. The first is that the Zeeman splitting energies of the hole levels localized at the interface region and confined in the quantum well have different values; this is related to the well-known dependence of g factor on the strength of the confining potential. The second point concerns the *spin-flip* mechanism during tunneling and relaxation processes. In the presence of *spin-flip*, if holes confined in the accumulation layer had the same g factor as, for instance, in the HH_2 QW level, we should observe three current peaks: one single resonance peak at the voltage where both *spin-up* and *spin-down* levels become simultaneously resonant and two other adjacent smaller peaks corresponding to *spin-flip* tunneling processes: up $\rightarrow$ down and down $\rightarrow$ up. In contrast, for different g factors in the layers, the resonance should result in four peaks: two strong peaks at different resonant voltages for *spin-up* and *spin-down*, plus the two additional weak peaks when *spin-flip* processes are present. The splitting of the HH_2 level into one doublet structure, which is not well resolved as shown in Fig. 3(a), could provide some evidence that the holes in the accumulation and QW layers have different g-factor values and that *spin-flip* processes have a negligible probability.

In principle, it is difficult to calculate or measure the g factors of excited levels. Our simulation only provides effective values for the difference between the g values that best represent our experimental data. The unknown g parameters

for any doublet carrier level are determined during the simulation for the resonant injection condition at the respective bias values. It becomes difficult to assign specific values for these carriers since the reported values[14,16,17] are for *localized* states in a QW whereas our data refer to *delocalized* (extended) states in a RTD, in the presence of applied bias.

Finally, even though we have not obtained quantitative values for the carrier relaxation times, our experimental and theoretical results provide evidence that these characteristic time scales are larger than the luminescence decay time in our structure, which should be <1 ns.

Moreover, the agreement between our experimental results and the theoretical simulation, which neglects hole spin-decoherence processes, provides further evidence of hole spin relaxation times which are significantly longer than the tunneling and recombination times. These results are important for possible future applications since they demonstrate the possibility of developing hole-based spintronic devices. Despite the approximations in our model, it provides a simple and fairly accurate explanation for the observed bias dependence of the optical polarization from the E_1^+-HH_1^+ and E_1^--HH_1^- QW emissions.

In summary, we have investigated spin-polarized carrier injection in nonmagnetic RTD structures. A strong bias-dependent optical polarization, with sign inversions near the low-bias resonant peaks and with positive saturation in the high-voltage regime, is observed. We have proposed a simple model based on the dynamical balance between carrier injection and energy relaxation which describes the observed bias dependence of the PL polarization for the low- and high-voltage regimes. The main feature of our results is the efficient spin-selective tunneling into excited QW subbands followed by spin-conserving relaxation to the HH_1 and E_1 spin-split ground states. Our results demonstrate indirectly that the g factors and spin-coherence time of holes on a quantum well may assume large values due to the mixing of the hole subbands and confining potential. We also demonstrate voltage-controlled injection of spin-polarized holes into a QW using standard nonmagnetic semiconductor heterostructures. The high sensitivity and the bias dependence of the PL polarization, including the inversion of polarization near hole resonances, are direct manifestations of this possibility; efficient spin-polarized injection requires well-resolved Zeeman-split states. New devices based on nonmagnetic semiconductor structures can be designed to take advantage of these effects to work as efficient spin filters.

ACKNOWLEDGMENTS

The authors acknowledge financial support from the Brazilian agencies FAPESP and CNPq and from the U.K. Engineering and Physical Sciences Research Council. We also thank M. Maialle for helpful discussions on phonon relaxation.

*Also at Universidade Federal de Santa Catarina. Electronic address: yara@df.ufscar.br

[1] I. Zutic, J. Fabian, and S. Das Sarma, Rev. Mod. Phys. **76**, 323 (2004).
[2] O. Z. Karimov, G. H. John, R. T. Harley, W. H. Lau, M. E. Flatte, M. Henini, and R. Airey, Phys. Rev. Lett. **91**, 246601 (2003).
[3] G. Schmidt, D. Ferrand, L. W. Molenkamp, A. T. Filip, and B. J. van Wees, Phys. Rev. B **62**, R4790 (2000).
[4] E. I. Rashba, Phys. Rev. B **62**, R16267 (2000).
[5] A. Fert and H. Jaffrès, Phys. Rev. B **64**, 184420 (2001).
[6] A. Slobodskyy, C. Gould, T. Slobodskyy, C. R. Becker, G. Schmidt, and L. W. Molenkamp, Phys. Rev. Lett. **90**, 246601 (2003).
[7] R. Fiederling, M. Klein, G. Reuscher, W. Ossau, A. Waag, and L. W. Molenkamp, Nature (London) **402**, 787 (1999).
[8] B. Habib, E. Tutuc, S. Melinte, M. Shayegan, D. Wasserman, S. A. Lyon, and R. Winkler, Phys. Rev. B **69**, 113311 (2004).
[9] R. Winkler, Phys. Rev. B **69**, 045317 (2004).
[10] A. Vercik, Y. Galvão Gobato, A. C. Rodrigues Bittencourt, G. E. Marques, M. J. S. P. Brasil, and C. Trallero-Giner, J. Appl. Phys. **93**, 5830 (2003).
[11] M. Dobers, K. von Klitzing, G. Weimann, and W. Schlapp, Solid State Commun. **74**, 1441 (1990).
[12] X. Marie, T. Amand, P. Le Jeune, M. Paillard, P. Renucci, L. E. Golub, V. D. Dymnikov, and E. L. Ivchenko, Phys. Rev. B **60**, 5811 (1999).
[13] V. F. Sapega, M. Cardona, K. Ploog, E. L. Ivchenko, and D. N. Mirlin, Phys. Rev. B **45**, 4320 (1992).
[14] M. J. Snelling, G. P. Flinn, A. S. Plaut, R. T. Harley, A. C. Tropper, R. Eccleston, and C. C. Phillips, Phys. Rev. B **44**, 11345 (1991).
[15] M. J. Snelling, E. Blackwood, C. J. McDonagh, R. T. Harley, and C. T. B. Foxon, Phys. Rev. B **45**, R3922 (1992).
[16] A. Malinowski and R. T. Harley, Phys. Rev. B **62**, 2051 (2000).
[17] R. Winkler, S. J. Papadakis, E. P. De Poortere, and M. Shayegan, Phys. Rev. Lett. **85**, 4574 (2000).
[18] D. J. Hilton and C. L. Tang, Phys. Rev. Lett. **89**, 146601 (2002).
[19] M. Z. Maialle, Semicond. Sci. Technol. **13**, 852 (1998).
[20] T. Uenoyama and L. J. Sham, Phys. Rev. Lett. **64**, 3070 (1990).
[21] R. Mattana, J.-M. George, H. Jaffres, F. N. vanDau, A. Fert, B. Lepine, A. Guivarch, and G. Jezequel, Phys. Rev. Lett. **90**, 166601 (2003).
[22] P. Roussignol, P. Rolland, R. Ferreira, C. Delalande, G. Bastard, A. Vinattieri, J. Martinez-Pastor, L. Carraresi, M. Colocci, J. F. Palmier, and B. Etienne, Phys. Rev. B **46**, 7292 (1992).
[23] S. Bar-Ad and I. Bar-Joseph, Phys. Rev. Lett. **68**, 349 (1992).
[24] T. C. Damen, L. Vina, J. E. Cunningham, J. Shah, and L. J. Sham, Phys. Rev. Lett. **67**, 3432 (1991).
[25] R. K. Hayden, D. K. Maude, L. Eaves, E. C. Valadares, M. Henini, F. W. Sheard, O. H. Hughes, J. C. Portal, and L. Cury, Phys. Rev. Lett. **66**, 1749 (1991).
[26] S. J. Prado, V. López-Richard, A. M. Alcalde, and G. E. Marques, J. Phys.: Condens. Matter **16**, 6949 (2004).
[27] H. B. de Carvalho, M. J. S. P. Brasil, V. Lopez-Richard, I. Camps, Y. Galvão Gobato, G. E. Marques, L. C. O. Dacal, M. Henini, L. Eaves, and G. Hill, cond-mat/0601421 (unpublished).

[28] M. I. D'yakonov and V. I. Perel, Sov. Phys. Solid State **13**, 3023 (1972).

[29] G. E. Marques, A. C. R. Bittencourt, C. F. Destefani, and Sergio E. Ulloa, Phys. Rev. B **72**, 045313 (2005).

[30] R. K. Hayden, L. Eaves, M. Henini, D. K. Maude, J. C. Portal, and G. Hill, Appl. Phys. Lett. **60**, 1474 (1992).

[31] T. S. Turner, L. Eaves, C. R. H. White, M. Henini, and G. Hill, Semicond. Sci. Technol. **9**, 552 (1994).

[32] M. S. Skolnick, D. G. Hayes, P. E. Simmonds, A. W. Higgs, G. W. Smith, H. J. Hutchinson, C. R. Whitehouse, L. Eaves, M. Henini, O. H. Hughes, M. L. Leadbeater, and D. P. Halliday, Phys. Rev. B **41**, 10754 (1990).